

Head-to-head comparison of ^{68}Ga -prostate-specific membrane antigen PET/CT and ferumoxtran-10 enhanced MRI for the diagnosis of lymph node metastases in prostate cancer patients

Authors

Melline GM Schilham, MD^{1‡}, Patrik Zamecnik, MD^{1‡}, Bastiaan M Privé, MD¹, Bas Israël MD¹, M Rijpkema, PhD¹, Tom Scheenen, PhD¹, Jelle O Barentsz, MD, PhD¹, James Nagarajah, MD PhD^{1,2*} and Martin Gotthardt MD, PhD^{1*}

¹Department of Medical Imaging, Nuclear Medicine, Radboud University Medical Centre, Nijmegen, The Netherlands

²Department of Nuclear Medicine, Technical University Munich, Klinikum rechts der Isar, Munich, Germany

[‡]co-first authors

*co-senior authors

Corresponding and first author:

Melline GM Schilham MD, PhD candidate.

Department of Medical Imaging, Nuclear Medicine, Radboud University Medical Centre
Geert Grooteplein Zuid 10, 6525 GA Nijmegen, The Netherlands

Tel: +31 (0) 243690031

Email: melline.schilham@radboudumc.nl

Orchid ID: 000-0002-7267-1976

Wordcount 4948

Wordcount abstract: 348

Immediate Open Access: Creative Commons Attribution 4.0 International License (CC BY) allows users to share and adapt with attribution, excluding materials credited to previous publications.

License: <https://creativecommons.org/licenses/by/4.0/>.

Details: <https://jnm.snmjournals.org/page/permissions>.



FINANCIAL SUPPORT

Not applicable

DISCLOSURES

PZ has following conflict of interests: scientific advisor to SPL Medical B.V.; options in SPL Medical B.V.

JB is scientific advisor to SPL Medical B.V. All other authors declare no conflicts of interest.

Short running title:

Comparison of PSMA-PET/CT and nano-MRI

ABSTRACT

Accurate assessment of lymph node (LN) metastases in prostate cancer (PCa) patients is critical for prognosis and patient management. Both prostate-specific membrane antigen- (PSMA) positron emission tomography/computed tomography (PET/CT) and ferumoxtran-10 nanoparticle-enhanced magnetic resonance imaging (nano-MRI) are imaging modalities with high potential to identify LN metastases in PCa patients. The aim of this study is to compare the results of those imaging technologies in terms of characteristics and anatomical localisation of suspicious LNs in order to assess the feasibility of their complementary use for imaging in PCa patients.

Methods:

A total of 45 patients with either primary PCa (n=8) or recurrence (n=36) were included in this retrospective study. All patients underwent both PSMA-PET/CT and nano-MRI between October 2015 and July 2017 within a time frame of three weeks. Both scans were performed at the same institution according to local clinical protocols. All scans were analysed independently by experienced nuclear medicine physicians and radiologists. The size, anatomical location and Level of Suspicion (LoS) were determined for all visible LNs. Subsequently, the findings from PSMA-PET/CT and nano-MRI were compared, irrespective to a reference standard.

Results:

179 suspicious LNs were identified. Significantly more suspicious LNs per patient were detected by nano-MRI ($p<0.001$): 160 were identified in 33 patients by nano-MRI, versus 71 in 25 patients by PSMA-PET/CT. Of all suspicious LNs 108 were only identified by nano-MRI (60%), 19 (11%) were detected only by PSMA-PET/CT, and 52 (29%) were found by both methods. The mean size of the suspicious LNs as identified by nano-MRI was significantly smaller (5.3mm) than those detected by PSMA-PET/CT (6.0mm; $p=0.006$). Median LoS did not differ significantly. Both modalities identified suspicious LNs in all anatomical regions of the pelvis.

Conclusion:

Both modalities identified suspicious LNs which were missed by the other. Both modalities identified suspicious LNs in all anatomical regions of the pelvis, however nano-MRI appeared to be superior in detecting smaller suspicious LNs. These findings suggest a potential complementary role for nano-MRI to PSMA-PET/CT, however, since the clinical implications of the different results are not well established yet, further investigation in this complementary use is encouraged.

Key Words:

Prostate cancer, lymph node, prostate specific membrane antigen; ⁶⁸Ga-PSMA-PET/CT, ferumoxtran-10.

INTRODUCTION

Detecting lymph node (LN) metastases in prostate cancer (PCa) patients is critical for prognosis and patient management. The current gold standard to assess the LN status is extended pelvic LN dissection (ePLND). However, this procedure is invasive and associated with considerable morbidity (1). Previous research demonstrated that in a substantial number of patients (60-85%), LN metastases were located outside the ePLND template (2-4). This illustrates the demand and increasing role for non-invasive imaging techniques to detect LN metastases in PCa patients.

Since conventional imaging techniques i.e. computed tomography (CT) and magnetic resonance imaging (MRI) use only morphologic criteria for LN assessment and in PCa more than 60% of LN metastases are present in normal-sized LNs (<8mm), these techniques are of limited value in LN staging (5,6), leading to the development of advanced functional and molecular imaging techniques. Recently, prostate-specific membrane antigen (PSMA) based positron emission tomography (PET)/CT was introduced. PSMA is a cell-surface glycoprotein, which is overexpressed on >90% of PCa cells (7). Small molecules with high binding affinity to PSMA are labelled with positron-emitters to enable whole-body tumour detection using PET/CT. Whereas data on accuracy was predominantly based on retrospective research (8), recently large prospective research by Hofman et al. demonstrated sensitivity and specificity of 0.85 and 0.98, respectively, for both LN and distant metastases (9). The rapid implementation of this technique in several PCa-guidelines affirms the demand for accurate staging methods (10,11).

Another potential imaging modality for N-staging is MR-lymphography or nanoparticle-enhanced MRI (nano-MRI). In nano-MRI ultra-small super-paramagnetic iron oxide particles (ferumoxtran-10; Ferrotran[®]; SPL Medical BV, Nijmegen, The Netherlands) are used as contrast-agent. Through accumulation after intravenous drip infusion of these particles in normal lymphatic tissue, nano-MRI allows differentiation of metastatic LNs from benign LNs, irrespective of nodal size (5,12). Reported sensitivity and specificity in detection of LN metastases in PCa patients are 82% and 93%, respectively (12). A meta-analysis reported sensitivities up to 90% and specificities up to 96% for various cancers, including PCa (13).

Published data suggest that PSMA-PET/CT and nano-MRI are the imaging modalities with the highest reported accuracy to detect LN metastases (9,14,15). Since both modalities rely on different technical and biological features, it was hypothesised that a combined use could even improve LN detection. Therefore, the goal of this study was to investigate the feasibility of a potential complementary role for those imaging modalities by comparing their results in the same patient and identifying differences and similarities in detected LN characteristics, irrespective of a reference standard.

MATERIALS AND METHODS

Patient Population

45 patients were enrolled in this retrospective study. Prior to the database creation, the institutional review board approved this study and the requirement to obtain informed consent was waived (CMO2019.5810). The study included all patients with either primary PCa (n=8) or recurrent disease (n=36), who underwent both nano-MRI and PSMA-PET/CT in our centre, between October 2015 and July 2017. Both scans needed to be performed within three weeks for inclusion. Patient characteristics were retrospectively collected from medical files.

⁶⁸Ga-PSMA-HBED-CC PET/CT

⁶⁸Ga-PSMA-PET/CT was performed using an integrated PET/CT system (Biograph mCT 4-ring, 40-slice Time Of Flight PET/CT scanner, Siemens Healthcare, Erlangen Germany). For all patients, ⁶⁸Ga-PSMA-HBED-CC was manufactured by the Radboud Translational Medicine Facility. PET acquisition was four minutes per bed position for the pelvic area and three minutes for the rest of the body. A low dose CT (slice thickness 5.0mm) was acquired for attenuation correction and image co-registration. PET/CT images were reconstructed in three orientations (axial, coronal and sagittal). The administered dose of the tracer was 2 MBq/kg body weight and imaging was initiated after approximately 60 minutes incubation time.

Nano-MRI

All patients received ferumoxtran-10 (Ferrotran®; SPL Medical BV, Nijmegen, The Netherlands) intravenously in weight-adapted dosage of 2.6 mg/kg body weight 24-36 hours prior to the MRI scan. Ferumoxtran-10 was diluted in 100mL NaCl 0.9% solution and was administered via drip infusion using a Minisart NML 0.22 µm pore size filter (Minisart NML Syringe Filters 16534-k; Sartorius AG, Göttingen, Germany). The infusion was performed at a slow rate of 1 mL/min at the start, increasing to 4 mL/min. The infusion duration was approximately 45 minutes and supervised by radiologists. MRI was performed using a 3-Tesla MRI-scanner (MAGNETOM Skyra or Trio, Siemens Healthineers, Erlangen, Germany). Imaging area included the pelvis, reaching from pubic bone to the aortic bifurcation. The MR-protocol consisted of an isotropic 3D T1-weighted gradient echo sequence (TR: 6.5 ms; TE:2.5 ms; flip angle: 10°; spatial resolution: 0.9 mm isotropic) and an isotropic 3D iron-sensitive T2*-weighted gradient echo sequence with fat saturation (Multiple Echo Data Image Combination (MEDIC) with TR:21 ms; TE: 12 ms; 3 combined echoes; flip angle: 10°; spatial resolution: 0.85 mm isotropic).

Image Analysis

All PSMA-PET/CT exams were retrospectively reviewed by two certified nuclear physicians in consensus (M.G. and J.N.) and the nano-MRI images were independently reviewed by one experienced radiologist (P.Z.). For both modalities, the number, the anatomical location, and size of detected LNs were reported. The location was described according to preconfigured anatomical locations in the pelvis, consistent with clinical practice in our department. LN size was measured (mm) for the smallest axis. Additionally, all detectable LNs were classified with a Level of Suspicion (LoS) for both nano-MRI and PSMA-PET/CT. This classification is a 5-point likeliness scale for potential malignancy assessment which is used by nuclear physicians and radiologists in our centre. For nano-MRI, LoS was based on the signal intensity in the iron sensitive T2*-weighted MRI sequence and its distribution within the LN based on to the diagnostic description proposed by Anzai et al (*16*). LoS for PSMA-PET/CT was based on the proposed criteria of the PSMA-RADS classification by Rowe et al. (*17*). This evaluation comprised of a combination of tracer

uptake, location and size. In more detail: LNs with no tracer uptake given a LoS 1, defined as “high probability of being benign”. LNs with equivocal tracer uptake at sites atypical of PCa involvement (e.g. axillary, hilar) were given a LoS 2 “probably benign”. LNs with equivocal tracer uptake located at sites typical of PCa involvement, LNs with intense uptake in sites highly atypical in PCa (i.e. the likelihood of non-prostatic malignancies or other (benign) origins is high) or LNs without tracer uptake, but with pathological aspects suggestive of malignancy on anatomical imaging were defined as LoS 3 “equivocal”. LNs with clearly increased tracer uptake, located at sites typical of PCa involvement, but lacking definitive findings on anatomical imaging were LoS4 “probably malignant”. LoS 5 “high probability of being malignant” was given to LNs with intense tracer uptake, located at sites typical of PCa and corresponding pathological findings on anatomical imaging. For both modalities, LNs with a LoS ≥ 3 were considered suspicious and taken for statistical evaluation.

Outcome Measurements and Statistical Analysis

Statistical analyses were performed using SPSS version 25 (SPSS Inc., Chicago, IL, USA). Descriptive statistical methods were used to characterise the patient cohort. For continuous data, mean and standard deviation were reported. For categorical data median and interquartile range (IQR) were described. Only non-parametrical statistical tests (Mann Whitney-U test and Wilcoxon signed-rank test) were performed since all data was non-normally distributed. A p-value of <0.05 was considered statistically significant.

RESULTS

45 patients underwent nano-MRI and ^{68}Ga -PSMA-PET/CT within a mean of 3 days (range 1-18 days) between October 2015 and July 2017. The mean age of the patients was 64 years (range 48-82 years). For the total cohort, mean prostate specific antigen (PSA) level at the time of scanning was 9.9 ng/ml (range 0.1-150 ng/ml). For the subgroup of patients who underwent imaging for primary staging (n=8), mean PSA was 28.9 ng/ml (range 5.6-150 ng/ml). The mean PSA-level in patients with recurrent disease (n=33) was

5.0 ng/ml (range 0.1-46 ng/ml). Detailed patient characteristics are described in Table 1. The median administered dose of ⁶⁸Ga-PSMA-HBED-CC was 158 MBq (IQR 133-180MBq).

A cumulative total of 179 suspected LNs (LoS ≥ 3) were identified in 33 patients. Examples of suspicious LNs as identified by nano-MRI, PSMA-PET/CT or both are shown in Figure 1a-c. Characteristics of the results of nano-MRI and PSMA-PET/CT are shown in Table 2. A total of 179 suspicious LNs were identified. Significantly more suspicious LNs were detected by nano-MRI ($p < 0.001$): 160 were identified in 33 patients by nano-MRI, versus 71 in 25 patients by PSMA-PET/CT. Thus, per patient nano-MRI identified significantly more suspicious LNs (mean 3.6, range 0-15) compared to PSMA-PET/CT (mean 1.6, range 0-12) ($p < 0.001$). The difference in size of the detected suspicious LNs by both modalities is shown in Figure 2. The mean size of the suspicious LNs identified by nano-MRI (5.2 mm, range 2-16) was significantly smaller compared to the mean size of suspicious LNs identified by PSMA-PET/CT (6.0 mm, range 3-16 mm) ($p = 0.006$).

Table 3 shows the conformity of both imaging modalities and demonstrates which LNs were identified by both modalities and which by only one. Of all suspicious LNs, most LNs were identified by nano-MRI alone ($n = 108$, 60%). Almost a third ($n = 52$, 29%) were identified by both modalities and 19 LNs (11%) were identified by PSMA-PET/CT alone. Not surprisingly, LNs identified by both modalities were larger (mean size 6.5mm, range 4-16mm) compared to LNs identified by either one of the modalities alone. In line with this finding is also the higher LoS of LNs identified by both modalities compared to LNs identified by one of the techniques alone.

An overview of the anatomical localisation of the suspicious LNs is depicted in Figure 3 (para-aortal, para-vesical LNs are left out). Both modalities identified LNs across all anatomical locations, either left or right sided. Remarkably, 43% ($n = 77$) of all detected suspicious LNs were located outside the standard ePLND resection field (included in ePLND: obturator, internal iliac, external iliac regions).

DISCUSSION

The aim of this study was to evaluate the feasibility of a complementary use of two high-precision imaging techniques for the detection of metastatic LNs in PCa patients. We hypothesised that a potential

complementary use could even improve LN detection. Therefore, we aimed to identify differences in terms of number, size, LoS and location of suspicious LNs, in order to determine the aspects where this complementary role would be most pronounced. In this direct comparative study, three important results were achieved. First, nano-MRI identified significantly more suspicious LNs per patient than PSMA-PET/CT ($p < 0.001$). Second, LNs identified by nano-MRI were significantly smaller ($p = 0.006$) compared to PSMA PET/CT. Third, both modalities identified LNs throughout the pelvis in all anatomical regions with, however, with a significant amount of suspicious LNs (43%) outside the standard ePLND templates.

To the best of our knowledge, this is the first study directly comparing these specific imaging techniques. In 2005-2006, Fortuin et al. conducted comparable research comparing nano-MRI with ^{11}C -choline-PET/CT. They showed a higher detection rate of small suspicious LNs by nano-MRI than ^{11}C -choline-PET/CT (18), a finding consistent with our results. In recent years, however, MRI has continued to develop and improve, and new technologies (PSMA-PET/CT) have emerged. To be more precise, technological improvements compared to the MRI-technique used by Fortuin et al. have led to even higher spatial resolution (2 mm compared to 4 mm) in MRI. Additionally, PSMA-based PET/CT has already proven to be more sensitive than choline-based PET/CT (19). Consequently, re-evaluation of these two imaging methods was considered valuable and led to the implementation of the current study.

Validation studies have already been conducted for both imaging modalities, showing promising results in terms of sensitivity and specificity, and as technological possibilities continue to evolve, accuracy is expected to improve further (9,12). Although there is no reference standard in this study, the main results mentioned above provide insight into the complementary performance of both modalities by identifying aspects where they agree and disagree. Such results allow the definition of future areas of research that need to be addressed in order to define the optimal imaging strategy for PCa patients.

Our results show a potentially higher detection rate for nano-MRI compared to PSMA-PET/CT. As Figure 2 shows, disagreement is most pronounced in LNs < 6 mm, suggesting size is the most likely explanation for this difference. Recent research demonstrated large differences in median histological size of metastatic LNs that were detected compared to LN metastases that were undetected by PSMA-PET/CT,

suggesting a size-related sensitivity for LN metastasis detection by PSMA-PET/CT (20,21). Possible explanations for this finding can be found in the biological properties of PSMA-expression on tumour tissue, as larger lesions are likely to have more PSMA-receptors and thus higher tracer uptake. Yet, PSMA-PET/CT could detect the smallest PSMA-positive lesions (below spatial resolution of the scanner) if PSMA-expression is highly concentrated, but could miss a larger lesion if PSMA-expression is too dispersed (20). Furthermore, it has been demonstrated that PSMA expression is correlated with tumour ISUP-grade group and serum PSA level (22,23). Additionally, about 5-10% of the PCa lesions do not express PSMA (7). Since the iron sensitive MRI sequence of nano-MRI has a higher spatial-resolution (isotropic resolution of 0.85 mm) compared to PET-CT (6 mm). The resolution of nano-MRI enables to detect LNs down to a size of 2mm^3 voxel size. Thus, in contrast to nano-MRI, the performance of LN detection by PSMA-PET/CT is largely dependent on tumour biology (24). From this, it could be anticipated that there is a potential advantage of nano-MRI in PCa patients with lower ISUP-grade group and PSA-values. In order to draw solid conclusions from this disagreement regarding small suspicious LNs, more research is needed with regard to the clinical significance of those small, potentially metastatic LNs and the biology of PSMA-expression.

The difference in pathophysiological targets between both modalities (PSMA-expression *versus* lymphatic invasion of tumour tissue) could also partly explain our finding that nano-MRI identified suspicious LNs in eight patients (8/45, 18%) without any suspicious LN on PSMA-PET/CT. This finding suggests either false-positive LNs for nano-MRI or a false-negative rate for PSMA-PET/CT or, most likely, a combination of both. Based on the mentioned different pathophysiological targets there are multiple explanations. Since about 5-10% of tumour lesions do not show PSMA expression, these lesions will be missed by PSMA-PET/CT (7). As sensitivity of PSMA-PET/CT in essence depends on PSMA-expression, this could explain the failing of the detection of lesions with a too low PSMA-expression level. On the other hand, nano-MRI relies on lymphotropic affinity of ferumoxtran-10 by macrophages, which accumulate the contrast agent in healthy LNs. Thus, in case of disturbance of accumulation in non-metastatic tissue, e.g. by fibrosis, the discriminative ability between metastatic and non-metastatic tissue in nano-MRI

could be impaired. Ideally, a reference standard should be used to evaluate those results and such research is strongly encouraged, but this surpasses the scope of the current study.

Contrary to the disagreement in size-related detection rates, another important finding was the agreement on anatomical localisation; there were no anatomical regions in which either modality could not detect suspicious LNs (Figure 3). In addition, both modalities identified a substantial amount of suspicious LNs outside the e-PLND template (total 77/179, 43%). This finding is also described in recent research (12,25,26) and has major impact on clinical care, as it challenges the diagnostic and therapeutic value of ePLND (27). This emphasizes the importance of accurate imaging modalities and explains the current rapidly changing of clinical guidelines since the introduction of PSMA-PET/CT (9,28).

This study was not without limitations. An important limitation of the study is its retrospective nature. Also, the studied population was relatively small and heterogeneous, as it consisted of both patients in the primary setting as well as biochemically recurrent setting. However, this was due to the limited number of patients who underwent both scans within a sufficiently tight time-frame. Although the number of patients is limited, the population is unique and allowed us to compare the diagnostic performance of these imaging techniques without the disruptive effect of anatomical discordances. A final limitation is the lack of histopathologic confirmation of the identified suspicious LNs. Unfortunately, histologic or clinical confirmation of the positive LNs was impossible since the majority of our patient group as presented was from abroad. Yet, the aim of this study was to compare the findings of both imaging modalities and discuss a potential clinical and scientific value (feasibility) of a complementary use, rather than validate their findings.

CONCLUSION

This study aimed to evaluate the feasibility of a combined role for PSMA-PET/CT and nano-MRI by comparing the results of those promising imaging modalities in the same population. In conclusion, the findings of this comparison study imply potential benefit from a complementary use of both modalities,

most pronounced in small LNs. In order to make clinical recommendations for such complementary use, more profound prospective research on the comparative results is warranted and should focus on size-related issues and tumour biology (PSMA). Nevertheless, the results of this study underline the importance of understanding both the technical capabilities of imaging techniques in combination with tumour biology in order to interpret the imaging results appropriately.

KEY POINTS

QUESTION:

How do the imaging results of PSMA-PET/CT and nano-MRI compare in the same patients?

PERTINENT FINDINGS:

In this retrospective, head-to-head comparison study, comprising 45 patients, nano-MRI identified significantly more suspicious LNs per patient (mean 3.6) compared to PSMA-PET/CT (mean 1.6) and the mean size of LNs detected by nano-MRI (mean 5.3mm) was significantly smaller compared to PSMA-PET/CT (mean 6.0mm). Both modalities identified suspicious LNs in all anatomical pelvic regions.

IMPLICATIONS FOR PATIENT CARE:

The present study provides insight in the comparability of two highly promising imaging modalities in PCa patients, which may contribute to improved interpretation of their results.

FINANCIAL SUPPORT

Not applicable

DISCLOSURES

PZ has following conflict of interests: scientific advisor to SPL Medical B.V.; options in SPL Medical B.V. JB is scientific advisor to SPL Medical B.V. All other authors declare no conflicts of interest.

ACKNOWLEDGEMENTS

We thank Robin Merkx, MD for his contribution to drawing Figure 3 in this manuscript.

References

1. Fossati N, Willemse PM, Van den Broeck T, et al. The benefits and harms of different extents of lymph node dissection during radical prostatectomy for prostate cancer: A systematic review. *Eur Urol.* 2017;72:84-109.
2. Joniau S, Van den Bergh L, Lerut E, et al. Mapping of pelvic lymph node metastases in prostate cancer. *Eur Urol.* 2013;63:450-458.
3. Heesakkers RA, Jager GJ, Hövels AM, et al. Prostate cancer: detection of lymph node metastases outside the routine surgical area with ferumoxtran-10-enhanced MR imaging. *Radiology.* 2009;251:408-414.
4. Larbi A, Dallaudière B, Pasoglou V, et al. Whole body MRI (WB-MRI) assessment of metastatic spread in prostate cancer: Therapeutic perspectives on targeted management of oligometastatic disease. *Prostate.* 2016;76:1024-1033.
5. Harisinghani MG, Barentsz J, Hahn PF, et al. Noninvasive detection of clinically occult lymph-node metastases in prostate cancer. *N Engl J Med.* 2003;348:2491-2499.
6. Hovels AM, Heesakkers RA, Adang EM, et al. The diagnostic accuracy of CT and MRI in the staging of pelvic lymph nodes in patients with prostate cancer: a meta-analysis. *Clin Radiol.* 2008;63:387-395.
7. Silver DA, Pellicer I, Fair WR, Heston WD, Cordon-Cardo C. Prostate-specific membrane antigen expression in normal and malignant human tissues. *Clin Cancer Res.* 1997;3:81-85.
8. Perera M, Papa N, Roberts M, et al. Gallium-68 prostate-specific membrane antigen positron emission tomography in advanced prostate cancer—updated diagnostic utility, sensitivity, specificity, and distribution of prostate-specific membrane antigen-avid lesions: A systematic review and meta-analysis. *Eur Urol.* 2020;77:403-417.
9. Hofman MS, Lawrentschuk N, Francis RJ, et al. Prostate-specific membrane antigen PET-CT in patients with high-risk prostate cancer before curative-intent surgery or radiotherapy (proPSMA): a prospective, randomised, multicentre study. *Lancet.* 2020;395:1208-1216.
10. Maurer T, Eiber M, Schwaiger M, Gschwend JE. Current use of PSMA-PET in prostate cancer management. *Nat Rev Urol.* 2016;13:226-235.
11. Maurer T, Murphy DG, Hofman MS, Eiber M. PSMA-PET for lymph node detection in recurrent prostate cancer: How do we use the magic bullet? *Theranostics.* 2017;7:2046-2047.

12. Heesakkers RA, Hovels AM, Jager GJ, et al. MRI with a lymph-node-specific contrast agent as an alternative to CT scan and lymph-node dissection in patients with prostate cancer: a prospective multicohort study. *Lancet Oncol.* 2008;9:850-856.
13. Wu L, Cao Y, Liao C, Huang J, Gao F. Diagnostic performance of USPIO-enhanced MRI for lymph-node metastases in different body regions: a meta-analysis. *Eur J Radiol.* 2011;80:582-589.
14. Pfister D, Porres D, Heidenreich A, et al. Detection of recurrent prostate cancer lesions before salvage lymphadenectomy is more accurate with (68)Ga-PSMA-HBED-CC than with (18)F-Fluoroethylcholine PET/CT. *Eur J Nucl Med Mol Imaging.* 2016;43:1410-1417.
15. Fortuin A, Rooij M, Zamecnik P, Haberkorn U, Barentsz J. Molecular and functional imaging for detection of lymph node metastases in prostate cancer. *Int J Mol Sci.* 2013;14:13842-13875.
16. Anzai Y, Piccoli CW, Outwater EK, et al. Evaluation of neck and body metastases to nodes with ferumoxtran 10-enhanced MR imaging: phase III safety and efficacy study. *Radiology.* 2003;228:777-788.
17. Rowe SP, Pienta KJ, Pomper MG, Gorin MA. Proposal for a Structured Reporting System for Prostate-Specific Membrane Antigen-Targeted PET Imaging: PSMA-RADS Version 1.0. *J Nucl Med.* 2018;59:479-485.
18. Fortuin AS, Deserno WM, Meijer HJ, et al. Value of PET/CT and MR lymphography in treatment of prostate cancer patients with lymph node metastases. *Int J Radiat Oncol Biol Phys.* 2012;84:712-718.
19. Afshar-Oromieh A, Zechmann CM, Malcher A, et al. Comparison of PET imaging with a (68)Ga-labelled PSMA ligand and (18)F-choline-based PET/CT for the diagnosis of recurrent prostate cancer. *Eur J Nucl Med Mol Imaging.* 2014;41:11-20.
20. Jilg CA, Drendel V, Rischke HC, et al. Detection rate of (18)F-Choline PET/CT and (68)Ga-PSMA-HBED-CC PET/CT for prostate cancer lymph node metastases with direct link from PET to histopathology: dependence on the size of tumor deposits in lymph nodes. *J Nucl Med.* 2019;60:971-977.
21. Klingenberg S, Jochumsen MR, Ulhøi BP, et al. (68)Ga-PSMA PET/CT for primary NM staging of high-risk prostate cancer. *J Nucl Med.* 2020;EPub ahead of print.
22. Afshar-Oromieh A, Avtzi E, Giesel FL, et al. The diagnostic value of PET/CT imaging with the (68)Ga-labelled PSMA ligand HBED-CC in the diagnosis of recurrent prostate cancer. *Eur J Nucl Med Mol Imaging.* 2015;42:197-209.

- 23.** Privé BM, Israël B, Schilham MGM, et al. Evaluating F-18-PSMA-1007-PET in primary prostate cancer and comparing it to multi-parametric MRI and histopathology. *Prostate Cancer Prostatic Dis.* 2020.
- 24.** Perera M, Papa N, Christidis D, et al. Sensitivity, Specificity, and Predictors of Positive (68)Ga-Prostate-specific Membrane Antigen Positron Emission Tomography in Advanced Prostate Cancer: A Systematic Review and Meta-analysis. *Eur Urol.* 2016;70:926-937.
- 25.** Koerber SA, Stach G, Kratochwil C, et al. Lymph node involvement in treatment-naive prostate cancer patients: correlation of PSMA PET/CT imaging and Roach formula in 280 men in radiotherapeutic management. *J Nucl Med.* 2020;61:46-50.
- 26.** Meijer HJ, Fortuin AS, van Lin EN, et al. Geographical distribution of lymph node metastases on MR lymphography in prostate cancer patients. *Radiother Oncol.* 2013;106:59-63.
- 27.** Bravi CA, Fossati N, Gandaglia G, et al. Long-term Outcomes of Salvage Lymph Node Dissection for Nodal Recurrence of Prostate Cancer After Radical Prostatectomy: Not as Good as Previously Thought. *European Urology.* 2020;78:661-669.
- 28.** Fendler WP, Eiber M, Beheshti M, et al. (68)Ga-PSMA PET/CT: Joint EANM and SNMMI procedure guideline for prostate cancer imaging: version 1.0. *Eur J Nucl Med Mol Imaging.* 2017;44:1014-1024.

TABLES AND FIGURES

TABLE 1. Patient characteristics

Characteristic	Data	
Patients, n	45	
Age, years		
Mean (range)	64	(48-82)
Serum PSA level, ng/ml*		
Overall mean (range), <i>n</i> =42	9.9	(0.0-150)
Mean primary setting (range), <i>n</i> =8	28.9	(5.6-150)
Mean recurrence setting (range), <i>n</i> =33	5.0	(0.0-46)
Time between diagnosis and scans, months[†]		
Mean (range)	50	(1-202)
Time between scans, days		
Mean (range)	3.0	(1-18)
<i>Prior to imaging:</i>		
Any PCa treatment, n(%)		
Yes	36	(80)
No	8	(18)
Unknown	1	(2)
PLND		
Yes	22	(49)
No	19	(42)
Unknown	4	(9)
Clinical ISUP grade		
ISUP 1	5	(11)
ISUP 2	6	(13)
ISUP 3	7	(16)
ISUP 4	13	(29)
ISUP 5	8	(18)
Unknown	6	(13)

*No data available in 3 patients. [†]No data available in 1 patient.
 ISUP = International Society of Urological Pathology; PCa = prostate cancer; PLND = pelvic lymph node dissection;
 PSA = prostate specific antigen.

TABLE 2. Node detection and characteristics for nano-MRI and PSMA-PET/CT

Characteristic	Total		nano-MRI		PSMA-PET/CT		<i>p-value</i>
Total scans (n)	90		45		45		
Total positive scans, n(%)	58	(64)	33	(73)	25	(56)	
Total suspicious LN, n(%)	179 (100)		160 (89)		71 (40)		
Suspicious LN/patient (n)							
Mean (range)	4.0	(0-6)	3.6	(0-15)	1.6	(0-12)	<0.001*
Suspicious LN size (mm)							
Mean (range)	5.2	(2-16)	5.3	(2-16)	6.0	(3-16)	0.006 [†]
LoS							
Median (IQR)	4	(4-5)	4	(4-5)	5	(4-5)	

* Positive scan defined as at least one LN with LoS ≥ 3 . [†]Wilcoxon signed-rank test; [‡]Mann-Whitney U test; IQR = inter-quartile range; LoS = level of suspicion; LN = lymph node; nano-MRI = nanoparticle-enhanced MRI; PET/CT = positron emission tomography/computed tomography; PSMA = prostate specific membrane antigen.

TABLE 3. Conformity of nano-MRI and PSMA-PET/CT.

Characteristic	<i>Suspicious LNs as detected by:</i>					
	Both nanoMRI & PSMA-		nano-MRI Only		PSMA-PET/CT only	
No. of patients (scans), n	20		30		14	
Total suspicious LNs, n (%)	52	(29)	108	(60)	19	(11)
Suspicious LNs/patient						
Mean (range)	1.2	(0-10)	2.4	(0-8)	0.4	(0-3)
LN size, mm						
Mean (range)	6.5	(4-16)	4.7	(2-16)	4.4	(3-8)
LoS						
Median (IQR)	5	(4-5)	4	(4-5)	3	(3-4)

IQR = interquartile range; LoS = level of suspicion; LN = lymph node; nano-MRI = nanoMRI; PET/CT = positron emission tomography; PSMA = prostate specific membrane antigen.

Figure Legends

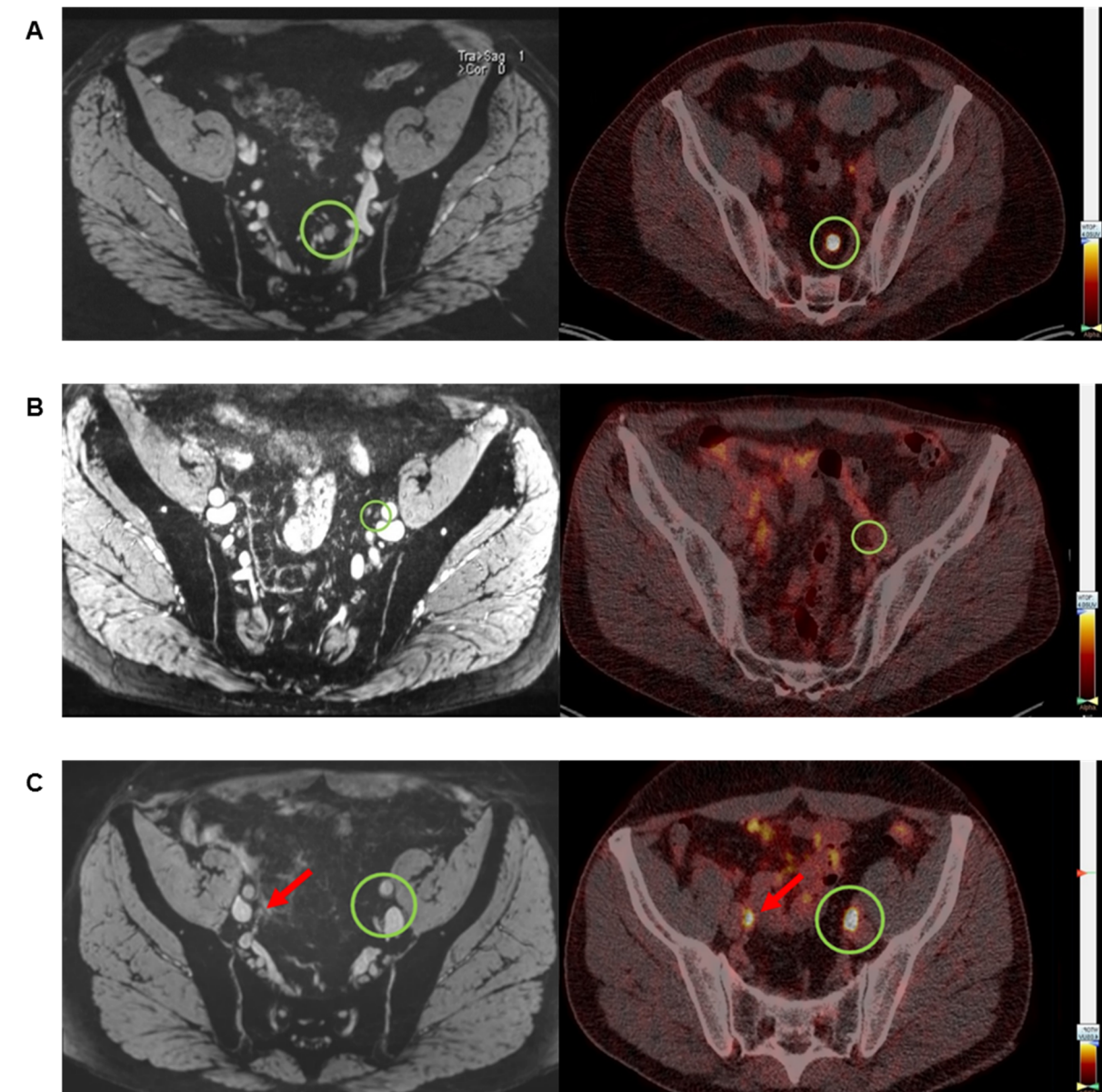


FIGURE 1. Three examples of suspicious lymph nodes (LNs) detected by either both modalities, nanoparticle-enhanced MRI (nano-MRI) alone and prostate-specific membrane antigen PET/CT (PSMA-PET/CT) alone. (A) Example of a LN which is positive on both nano-MRI (left image, iron sensitive T2* fat-saturated sequence) and PSMA-PET/CT; left pararectal region, LN diameter 7 mm. (B) Example of a LN which is positive on nano-MRI (left image, iron sensitive T2* fat-saturated sequence; a. iliaca externa region, diameter 4 mm, green circle) but negative on PSMA-PET/CT (right image). No tracer uptake in this region (green circle). (C) Example of a suspicious LN which is negative on nano-MRI (left image, iron sensitive T2* fat-saturated sequence, there is also no ureter visible in this area), but positive on PSMA-PET/CT (right image, green circle; dorsal of the a. iliaca externa left); Red arrows are showing the position of the right ureter.

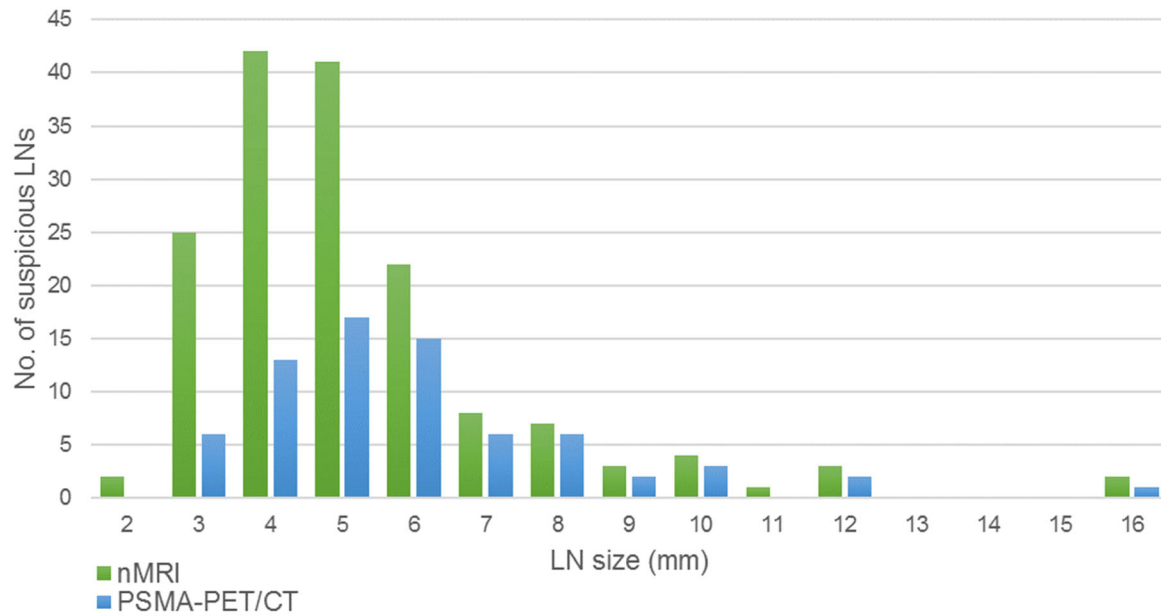


FIGURE 2. Size distribution of suspicious lymph nodes as detected by nanoparticle-enhanced MRI (green) and prostate-specific membrane antigen PET/CT (blue).

LN = lymph node; PSMA-PET/CT = prostate-specific membrane antigen positron emission tomography/computed tomography; nano-MRI = nanoparticle-enhanced magnetic resonance imaging.

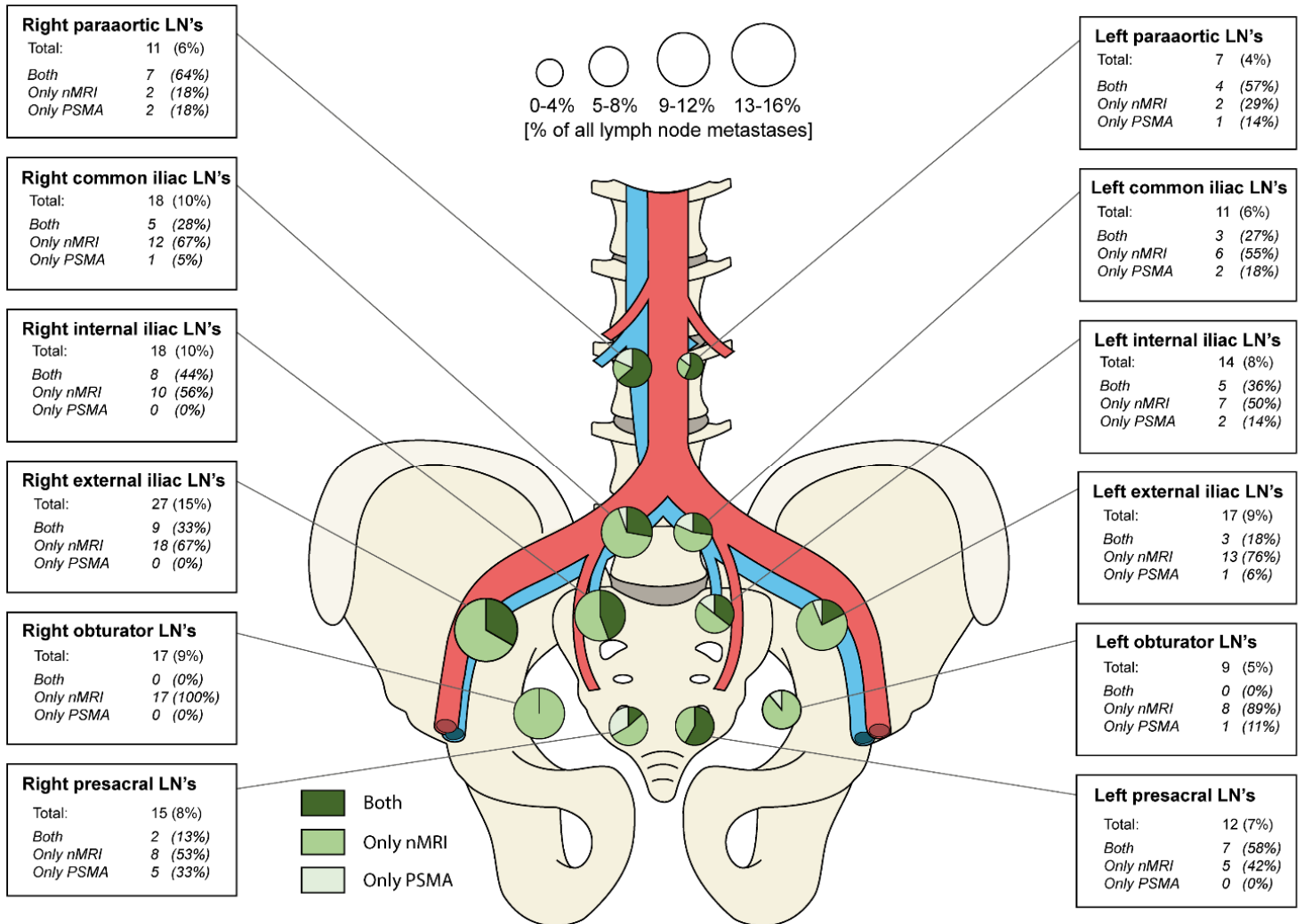


FIGURE 3. Anatomic distribution of identified suspicious lymph nodes as detected by nanoparticle-enhanced MRI and prostate-specific membrane antigen PET/CT.

LN = lymph node; PSMA-PET/CT = prostate-specific membrane antigen positron emission tomography/computed tomography; nano-MRI = nanoparticle-enhanced magnetic resonance imaging.

Graphical Abstract

